

Recreational Mathematics Magazine

Number 7
May, 2017



DE GRUYTER
OPEN



Ludus



CIUHCT

Games and Puzzles

EXPLORING THE “RUBIK’S MAGIC” UNIVERSE

Maurizio Paolini

Dipartimento di Matematica e Fisica, Università Cattolica “Sacro Cuore”, Brescia, Italy

paolini@dmf.unicatt.it

Abstract: *By using two different invariants for the Rubik’s Magic puzzle, one of metric type, the other of topological type, we can dramatically reduce the universe of constructible configurations of the puzzle. Finding the set of actually constructible shapes remains however a challenging task, that we tackle by first reducing the target shapes to specific configurations: the octominoid 3D shapes, with all tiles parallel to one coordinate plane; and the planar “face-up” shapes, with all tiles (considered of infinitesimal width) lying in a common plane and without superposed consecutive tiles. There are still plenty of interesting configurations that do not belong to either of these two collections. The set of constructible configurations (those that can be obtained by manipulation of the undecorated puzzle from the starting situation) is a subset of the set of configurations with vanishing invariants. We were able to actually construct all octominoid shapes with vanishing invariants and most of the planar “face-up” configurations. Particularly important is the topological invariant, of which we recently found mention in [7] by Tom Verhoeff.*

Keywords: Rubik’s Magic puzzle, octominoid 3D shapes, topological invariants.

Introduction

The *Rubik’s Magic* is another creation of Ernő Rubik, the brilliant hungarian inventor of the ubiquitous “cube” that is named after him. The *Rubik’s Magic* puzzle is much less known and not very widespread today, however it is a really surprising object that hides aspects which makes it quite an interesting subject for a mathematical analysis on more than one level.

We investigate here two different invariants that can be used to prove the unreachability of many spatial configurations of the puzzle, one of these invariants, of topological type, is to our knowledge never been extensively studied before, although it is presumably the same mentioned in [7], and allows to

significantly reduce the number of theoretically constructible shapes. However even in the special case of planar “face-up” configurations (see Section 8) we don’t know whether the combination of the two invariants, together with basic constraints coming from the mechanics of the puzzle, is complete, *i.e.* if it characterizes the set of constructible configurations. Indeed there are still a few planar face-up configurations having both vanishing invariants, but that we are not able to construct. In this sense this Rubik’s invention remains an interesting subject of mathematical analysis.

In Section 2 we describe the puzzle and discuss its mechanics, the local constraints are discussed in Section 3. The addition of a ribbon (Section 4) allows to introduce the two invariants, the metric and the topological invariants, described respectively in Sections 5 and 6.

The set of *octominoid* shapes (all tiles are parallel to a coordinate plane and no two of them are superposed) is described in Section 7. There are a total of 460 distinct octominoid configurations of the undecorated puzzle with vanishing invariants and **all** of them are actually constructible with the real puzzle [4, 3D octominoids] meaning that within this special class of shapes the two invariants are complete.

The special “face-up” planar configurations are defined in Section 8 and their invariants computed in Section 9. There are a total of 25 configurations with vanishing invariants, all of which we were able to actually construct [4, planar face-up configurations] with only 5 exceptions (Section 10). The two basic configurations of Figures 1 and 2 are contained in both octominoid and planar face-up classes, for a total of 485 configurations. Of course there are still many configurations that are not contained in either of the two classes (actually there are infinitely many of them), making the exploration of the Rubik’s Magic universe far from complete.

We conclude the paper with a brief description of the software codes used to help in the analysis of the octominoid and of the planar face-up configurations (Section 11).

The puzzle

The *Rubik’s Magic* puzzle (see Figure 1 left) consists of 8 decorated square tiles positioned to form a 2×4 rectangle.

They are ingeniously connected to each other by means of nylon strings lying in grooves carved on the tiles and tilted 45 degrees [2].

The tiles are decorated in such a way that on one side of the 2×4 original configuration we can see the picture of three unconnected rings, whereas on the back side we find non-matching drawings representing parts of rings with crossings among them.

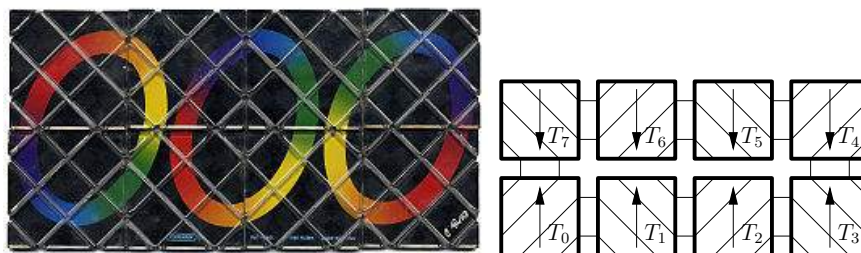


Figure 1: The original puzzle in its starting configuration (left). Orientation scheme for the tiles (right).



Figure 2: The puzzle in its target configuration, the tiles are turned over with respect to Figure 1.

The declared aim is to manipulate the tiles in order to correctly place the decorations on the back, which can be done only by changing the global outline of the eight tiles.

The solved puzzle is shown in Figure 2 with the tiles positioned in a 3×3 square with a missing corner and overturned with respect to the original configuration of Figure 1.

Detailed instructions on how the puzzle can be solved and more generally on how to construct interesting shapes can be copiously found in the internet, we just point to the Wikipedia entry [1] and to the web page [2]. The booklet [3] contains a detailed description of the puzzle and illustrated instructions on how to obtain particular configurations.

The decorations can be used to distinguish a “front” and a “back” face of each tile and to orient them by suitably choosing an “up” direction.

After dealing with the puzzle for some time it becomes apparent that a few local constraints are always satisfied. In particular the eight tiles remain always connected two by two in such a way to form a cyclic sequence. To fix ideas let

us denote the eight tiles by T_0, T_1, \dots, T_7 , with T_0 the lower-left tile in Figure 1 and the others numbered in counterclockwise order. For example tile T_3 is the one with the Rubik’s signature in its lower-right corner (see Figure 1).

With this numbering tile T_i is always connected through one of its sides to both tiles T_{i+1} and T_{i-1} . Here and in the rest of this paper we shall always assume the index i in T_i to be defined “modulo 8”, *i.e.* that for example T_8 is the same as T_0 .

We shall conventionally orient the tiles such that in the initial configuration of Figure 1 all tiles are “face up” (*i.e.* with their front face visible), the 4 lower tiles (T_0 to T_3) are “straight” (not upside down), the 4 upper tiles (T_4 to T_7) are “upside down” (as a map with the north direction pointing down), see Figure 1 right.

At a more accurate examination it turns out that only half of the grooves are actually used (those having the nylon threads in them). These allow us to attach to a correctly oriented tile (face up and straight) a privileged direction: direction \diagup (“slash”: North-East to South-West) and direction \diagdown (“backslash”: North-West to South-East). The used grooves are shown in Figure 1 right. From now on we shall disregard completely the unused grooves. In the initial configuration tiles T_i with even i are all tiles of type \diagup , whereas if i is odd we have a tile of type \diagdown .

The direction of the used grooves in the back of a tile is opposite (read orthogonal) to the direction of the used grooves of the front face, but beware that when we revert (turn over) a tile a \diagup groove becomes \diagdown , so that the reversed tile remains of the same type (\diagup or \diagdown).

From the point of view of an idealized physical modelling a natural choice would be to assume that the tiles are made of a rigid material and have infinitesimal thickness, and that the nylon threads are perfectly flexible but inextensible (and of infinitesimal thickness). This allows for two or more tiles to be juxtaposed in space, however in such a case we still need to retain the information about their relative position (which is above which).

However in this model there are moves that can be performed on the real puzzle (that entail a small amount of elongation on the nylon wires) but that are **not** allowed in the ideal model (see *e.g.* the two interesting shapes denoted *armchair* and *hard-to-reach planar shape* linked from 4).

For this reason in the real constructions we shall allow for moves that entail a small amount of deformation of the tiles and elongation of the wires. We shall not be rigorous about what is allowed and what is not, the rule being that we shall generally allow for moves that can actually be performed on the real puzzle.

On the contrary the real puzzle has non-infinitesimal tile thickness, which can lead to configurations that are alright for the idealized physical model but that are difficult or impossible to achieve (because of the imposed stress on the nylon threads) with the real puzzle.

Undecorated puzzle

We are here mainly interested in the study of the *shapes* in space that can be obtained, so we shall neglect the decorations on the tiles and only consider the direction of the grooves containing the nylon threads. In other words we only mark one diagonal on each face of the tiles, one connecting two opposite vertices on the front face and the other connecting the remaining two vertices on the back face.

Now the tiles (marked with these two diagonals) are indistinguishable; distinction between \boxplus and \boxminus is only possible after we have “oriented” a tile and in such a case rotation of 90 degrees or a mirror reflection will exchange \boxplus with \boxminus .

Definition 1 (orientation). *A tile can be oriented by drawing on **one** of the two faces an arrow parallel to a side. We have thus eight different possible orientations. We say that two adjacent tiles are compatibly oriented if their arrows perfectly fit together (parallel and pointing to the same direction) when we ideally rotate one tile around the side on which they are hinged to make it juxtaposed to the other. There is exactly one possible orientation of a tile that is compatible with the orientation of an adjacent tile. A configuration of tiles is **orientable** if it is possible to orient all tiles such that they are pairwise compatibly oriented. For an orientable configuration we have eight different choices for a compatible orientation of the tiles.*

An example of compatible orientation of a configuration is shown in Figure [1](#) right, which makes the initial 2×4 configuration orientable. Once we have a compatible orientation for a configuration, we can classify each tile as \boxplus or \boxminus according to the relation between the orienting arrow and the marked diagonal: a tile is of type \boxplus if the arrow aligns with the diagonal after a clockwise rotation of 45 degrees, it is of type \boxminus if the arrow aligns with the diagonal after a counterclockwise rotation of 45 degrees. Two adjacent tiles are always of opposite type.

Definition 2. *A spatial configuration of the puzzle that is **not** congruent (also considering the marked diagonals) after a rigid motion with its mirror image will be called **chiral**, otherwise it will be called **achiral**. Note that a configuration is achiral if and only if it is mirror symmetric with respect to some plane.*

The initial 2×4 configuration is achiral since it is specularly symmetric with respect to a plane orthogonal to the tiles.

Definition 3. *We say that an orientable spatial configuration of the puzzle (without decorations) is **constructible** if it can be obtained from the initial 2×4 configuration through a sequence of admissible moves of the puzzle.*

Once we have identified all the constructible spatial configurations, we also have all constructible configurations of the decorated puzzle. This is a consequence

of the fact that all possible 2×4 configurations of the decorated puzzle are completely classified (see for example [2] or [3]).

We note here that all 2×4 configurations of the undecorated puzzle are congruent, however the presence of the marked diagonal might require a reversal of the whole configuration upside-down in order to obtain the congruence.

For chiral configurations (those that cannot be superimposed with their specular images) the following result is useful.

Theorem 1. *A spatial configuration of the undecorated puzzle is constructible if and only if its mirror image is constructible.*

Proof. If a configuration is constructible we can reach it by a sequence of moves of the puzzle starting from the initial 2×4 configuration. However the initial 2×4 configuration is specularly symmetric, hence we can perform the specular version of that sequence of moves to reach the specular image of the configuration that we are considering. \square

Local constraints

We now consider a version of the puzzle where in place of the usual decoration we draw arrows on the “front” face of the tiles as in Figure 1 right. The linking mechanism with the nylon threads is such that two consecutive tiles T_i and T_{i+1} are always “hinged” together through one of their sides. In particular, if we suitably orient T_i with its “front” face visible and “straight”, i.e. with the arrow visible and pointing up) and we rotate tile T_{i+1} such that its center is as far away as possible from the center of T_i (like an open book), then also T_{i+1} will have its arrow visible and

- **pointing up** if the two tiles are hinged through a vertical side (the right or left side of T_i);
- **pointing down** if the two tiles are hinged through a horizontal side (the top or bottom side of T_i).

The surprising aspect of the puzzle is that when we “close the book”, i.e. we rotate T_{i+1} so that it becomes superimposed with (stacked on or below) T_i , we than can “reopen the book” with respect to a different hinging side. The new hinging side is one of the two sides that are orthogonal to the original hinging side, which one depending on the type of the involved tiles (direction of the marked diagonals) and can be identified by the rule that the new side is not separated from the previous one by the “inner” marked diagonals. For example, if T_i is of type \boxtimes (hence T_{i+1} is of type \boxminus) and they are hinged through the right side of T_i (as T_0 and T_1 of Figure 1 right) then after closing the tiles by rotating T_{i+1} **up** around its left side and placing it on top of (stacked above) T_i , then we can reopen the tiles with respect to the bottom side. On the contrary, if we rotate **down** T_{i+1} , so that it becomes stacked below T_i (and the involved marked diagonal of T_i is the one on the back face), the new hinging side will be the upper side.

We remark that if a configuration does not contain superimposed consecutive tiles, then the hinging side of any pair of consecutive tiles is uniquely determined. If the tiles are (compatibly) oriented, then for each tile T_i we have a unique side (say East, North, West or South, in short E , N , W or S) about which it is hinged with the preceding tile T_{i-1} and a unique side (E , N , W or S) about which it is hinged with T_{i+1} . The two sides can be the same.

Definition 4. *For a given spatial oriented configuration of the (undecorated) puzzle without stacked consecutive tiles we say that a tile is*

straight *if the two hinging sides are opposite;*

curving *if the two hinging sides are adjacent (but not the same). In this case we can distinguish between tiles **curving left** and tiles **curving right** with the obvious meaning and taking into account the natural ordering of the tiles induced by the tile index;*

a flap *if it is hinged about the same side with both the previous and the following tile.*

Flaps

Flap tiles (those that, following Definition 4, have a single hinging side with the two adjacent tiles) require a specific analysis. The term “flap” is the same used in [3] and refers to the similarity with the flaps of an airplane, that can rotate about a single side.

Given an oriented configuration with a flap T_i , let us fix the attention to the three consecutive tiles T_{i-1} , T_i , T_{i+1} and ignore all the others. Place the configuration so that T_i is horizontal, with its front face up and the arrow pointing North, then rotate T_{i-1} and T_{i+1} at maximum distance from T_i so that they become reciprocally superimposed.

Now all three tiles have their front face up and we can distinguish between two situations:

Definition 5. *Tile T_i is an **ascending flap** if tile T_{i-1} is **below** tile T_{i+1} ; it is a **descending flap** in the opposite case. Tile T_i is a **horizontal ascending / descending flap** if it is hinged at a vertical side (a side parallel to the arrow indicating the local orientation of the flap tile), it is a **vertical ascending / descending flap** otherwise.*

The ribbon trick

In order to introduce the metric and the topological invariants we resort to a simple expedient: we insert a ribbon in between the tiles that more or less follows the path of the nylon threads. The ribbon is colored red on one side (front side) and blue in its back side and is oriented with longitudinal arrows printed along its length that allows to follow it in the positive or negative direction.

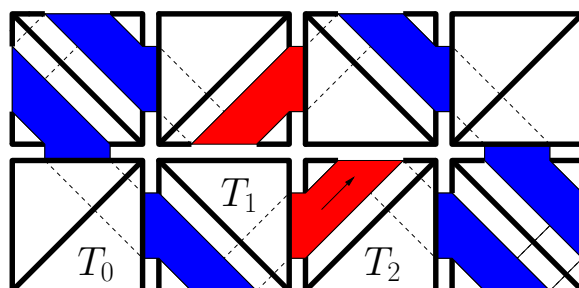


Figure 3: Ribbon path among the tiles.

Let the tiles have side of length 1, then the ribbon has width that does not exceed $\frac{\sqrt{2}}{4}$ (the distance between two nearby grooves), so that it will not interfere with the nylon threads. We insert the ribbon as shown in Figure 3. More precisely take the 2×4 initial configuration of the puzzle and start with tile T_2 . Position the ribbon such that it travels diagonally along the front face of T_2 as shown in Figure 3, then wrap the ribbon around the top side of T_2 and travel downwards along the back of T_2 to reach the right side. At this point we move from the back of T_2 to the front of T_3 (the ribbon now has its blue face up) and continue downward until we reach the bottom side of T_3 , wrap the ribbon on the back and so on.

In general, every time that the ribbon reaches a side of a tile that is not a hinge side with the following tile, we wrap it around the tile (from the front face to the back face or from the back face to the front face) as if it “bounces” against the side. Every time the ribbon reaches a hinging side of a tile with the following tile it moves to the next tile and crosses from the back (respectively front) side of one tile to the front (respectively back) side of the other and maintains its direction.

In all cases the ribbon travels with sections of length $\delta = \frac{\sqrt{2}}{2}$ between two consecutive “touchings” of a side. It can stay adjacent to a given tile during one, two or three of such δ steps: one or three if the tile is a *curving* tile (Definition 4), two if the tile is a *straight* tile.

After having positioned the ribbon along all tiles, it will close on itself nicely (in a straight way and with the same orientation) on the starting tile T_2 , and we tape it with itself. In this way the total length of the ribbon is 16δ with an average of 2δ per tile, moreover if we remove the ribbon without cutting it (by making the tiles “disappear”), we discover that we can deform it in space into the lateral surface of a large and shallow cylinder with height equal to the ribbon thickness and circumference 16δ .

Direct inspection also shows that the inserted ribbon does not impact on the possible puzzle moves, whereas its presence allows us to define the two invariants of Sections 5 and 6.

We remark a few facts:

1. The ribbon is oriented: it has arrows on it pointing in the direction in which we have inserted it, and while traversing the puzzle along the ribbon the tiles are encountered in the order given by their index.
2. Each time the ribbon “bounces” at the side of a tile (moving from the front face to the back face or viceversa) its direction changes of 90 degrees and simultaneously it turns over. This does not happen when the ribbon moves from one tile to the next, it does not change direction and it does not turn over.
3. Each δ section of the ribbon connects a horizontal side to a vertical side or viceversa; consequently the ribbon touches alternatively horizontal sides and vertical sides.
4. Each time the ribbon touches a lateral side it goes from one side of the tiles to the other (from the front to the back or from the back to the front).

The above points 3 and 4 prove the following

Proposition 2. *Following the orientation of the ribbon, when the ribbon touches/crosses a vertical side, it “emerges” from the back of the tiles to the front, whereas when it touches/crosses a horizontal side, it “submerges” from the front to the back. Here vertical or horizontal refers to the local orientation assigned to the tiles.*

Behaviour of the ribbon at a flap tile.

It is not obvious how the ribbon behaves at a flap tile (such tiles are not present in the initial 2×4 configuration). We can reconstruct the ribbon position by imagining a movement that transforms a configuration without flaps to another with one flap.

It turns out that there are two different situations. In one case the ribbon completely avoids to touch the flap tile T_i and directly goes from T_{i-1} to T_{i+1} , this happens when in a neighbourhood of the side where the flap tile is hinged the ribbon is on the front face of the upper tile and on the bottom face of the lower tile (in the configuration where T_{i-1} and T_{i+1} are furthest away from T_i , hence superposed), this situation is illustrated in Figure 4 left. In the other case the ribbon wraps around T_i with four δ sections alternating between the front face and the back face, this situation is illustrated in Figure 4 right.

The first of the two cases arises at an *ascending* flap hinged at a vertical side (horizontal ascending flap) or at a *descending* flap hinged at a horizontal side (vertical descending flap); this is independent of the type ∇ or \square of the flap tile.

The second of the two cases arises at a vertical ascending flap or at a horizontal descending flap.

Metric invariant

Whatever we do to the puzzle (with the ribbon inserted) there is no way to change the length of the ribbon!

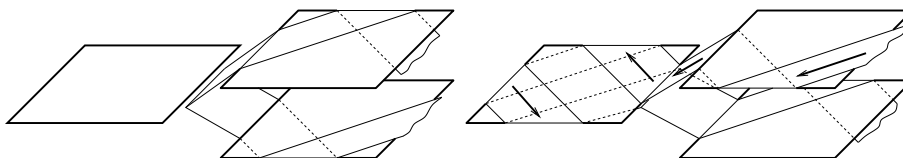


Figure 4: Position of the ribbon in presence of a “flap” tile. The flap tiles are of type \boxplus , The superposed tiles are all of type \boxminus . Left: ascending flap, the ribbon does not even touch the flap tile. Right: descending flap, the ribbon completely wraps the flap tile with four sections, two on the upper (front) face and two on the back face.

This allows to regard the length of the ribbon associated to a given spatial configuration as an invariant, it cannot change under puzzle moves. The computation of the ribbon length can be carried out by following a few simple rules, they can also be found in [3].

The best way to proceed is to compute for each tile T_i how many δ sequences of the ribbon wrap it and subtract the mean value 2. The resulting quantity will be called Δ_i and its value is:

- $\Delta_i = 0$ if T_i is a straight tile (Definition 4);
- $\Delta_i = -1$ if T_i is of type \boxminus and is “curving left”, or if it is of type \boxplus and is “curving right”;
- $\Delta_i = +1$ if T_i is of type \boxminus and is curving right, or if it is of type \boxplus and is curving left;
- $\Delta_i = -2$ if T_i is a horizontal ascending flap (Definition 5) or a vertical descending flap (see Figure 4 left);
- $\Delta_i = +2$ if T_i is a horizontal descending flap or a vertical ascending flap (see Figure 4 right).

The last two cases ($|\Delta_i| = 2$) follow from the discussion in Section 4.1.

We call $\Delta = \sum_{i=0}^7 \Delta_i$, the sum of all these quantities, then the total length of the ribbon will be $16\delta + \Delta\delta$ and hence Δ is invariant under allowed movements of the puzzle. Since in the initial configuration we would have $\Delta = 0$ it follows that

Theorem 3. *Any constructible configuration of the puzzle necessarily satisfies $\Delta = 0$.*

This invariant can also be found in [3, page 19], though it is not actually justified.

A few configurations (e.g. the 3×3 shape without the central square, called “window shape” in [3]) can be ruled out as non-constructible by computing the Δ invariant. The “window shape” has a value $\Delta = \pm 4$, the sign depending on how we orient the tiles. It is non-constructible because $\Delta \neq 0$. Figure 15 (left) shows a deformed version of this shape.

Another interesting configuration that can be ruled out using this invariant is sequence (7), to be discussed in Section 9.1.

Topological invariant

Sticking to the ribbon idea (Section 4) we seek a way to know whether a given ribbon configuration (with the tiles and nylon threads removed) can be obtained by deformations in space starting from the configuration where the ribbon is the lateral surface of a cylinder.

Topologically the ribbon is a surface with a boundary, its boundary consists of two closed strings.

One thing that we may consider is the center line of the ribbon: it is a single closed string that can be continuously deformed in space and is not allowed to cross itself. Mathematically we call this a “knot”, a whole branch of Mathematics is dedicated to the study of knots, one of the tasks being finding ways to identify “unknots”, i.e. tangled closed strings that can be “unknotted” to a perfect circle.

This is precisely our situation: the center line of the ribbon must be an unknot, otherwise the corresponding configuration of the puzzle cannot be constructed. However we are not aware of puzzle configurations that can be excluded for this reason.

Another (and more useful) idea consists in considering the two strings forming the boundary of the ribbon. In Mathematics, a configuration consisting in possibly more than one closed string is called a “link”. Here we have a two-components link that in the starting configuration can be deformed into two unlinked perfect circles.

There is a topological invariant that can be easily computed, the *linking number* between two closed strings, that does not change under continuous deformations of the link (again prohibiting selfintersections of the two strings or intersections of one string with the other).

In the original configuration of the puzzle, the two strings bordering the ribbon have linking number zero: it then must be zero for any constructible configuration.

Computing the linking number

In the field of *knot theory* a knot, or more generally a link, is often represented by its diagram. It consists of a drawing on a plane corresponding to some orthogonal projection of the link taken such that the only possible selfintersections are transversal crossings where two distinct points of the link project onto the same point. We can always obtain such a *generic* projection possibly by changing a little bit the projection direction. We also need to add at all crossings the information of what strand of the link passes “over” the other. This is usually done by inserting a small gap in the drawing of the strand that goes below the other, see Figure [5](#).

In order to define the linking number between two closed curves we need to select an orientation (a traveling direction) for the two curves.

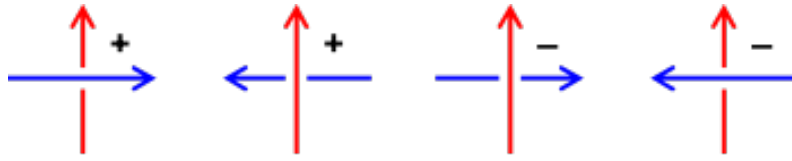


Figure 5: Signature of a crossing for the computation of the linking number.

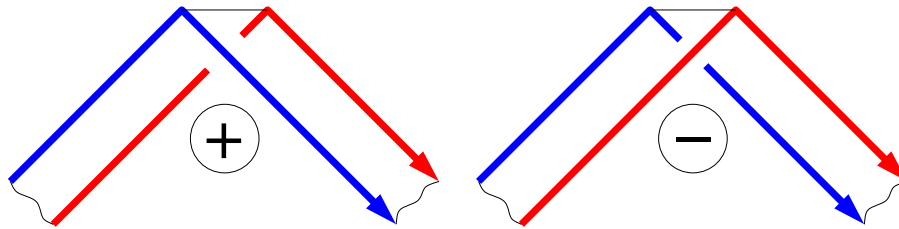


Figure 6: The ribbon *bounces* at the side of a tile.

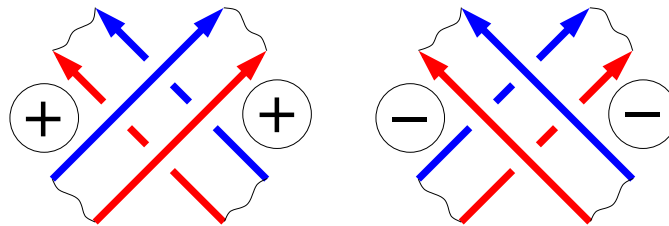


Figure 7: The ribbon passes over/below itself.

In our case the orientation of the ribbon induces an orientation of the two border strings by following the same direction. The linking number changes sign if we revert the orientation of one of the two curves, so that it becomes insensitive upon the choice of orientation of the ribbon. Once we have an orientation of the two curves, we can associate a signature to each crossing as shown in Figure 5 and a corresponding weight of value $\pm\frac{1}{2}$. Crossings of a component with itself are ignored in this computation.

The linking number is given by the sum of all these contributions. Since the number of crossings in between the two curves in the diagram is necessarily even, it follows that the linking number is an integer and it can be proved that it does not change under continuous deformations of the link in space. Two far away rings have linking number zero, two linked rings have linking number ± 1 .

In our case we shall investigate specifically the case where all tiles are horizontal and “face-up”, in which case we have two different situations that produce crossings between the two boundary strings. We shall then write the linking number as the sum of a “twist” part (L_t) and a “ribbon crossing” part (L_c)

$$L = L_t + L_c \quad (1)$$

where we distinguish the two cases:

1. The ribbon wraps around one side of a tile (Figure 6). This entails one crossing in the diagram, that we shall call “twist crossing” since it is actually produced by a twist of the ribbon. A curving tile (as of Definition 4) can contain only zero or two of this type of crossings, and if there are two, they are necessarily of opposite sign. This means that curving tiles do not contribute to L_t .
2. The ribbon crosses itself (Figure 7). Consequently there are four crossings of the two boundary strings, two of them are selfcrossings of one of the strings and do not count, the other two contribute with the same sign for a total contribution of ± 1 to L_c . The presence of this type of crossings is generally a consequence of the spatial disposition of the sequence of tiles and in the specific case of face-up planar configurations (to be considered in Section 8) there can be crossings of this type when we have superposed tiles, or in presence of flap tiles, however the computation of L_c must be carried out case by case.

Contribution of the straight tiles to L_t .

The ribbon “bounces” exactly once at each straight tile (Definition 4), hence it contributes to L_t with a value $\delta L_t = \pm \frac{1}{2}$.

After analyzing the various possibilities we conclude for tile T_i as follows:

- $\delta L_t = +\frac{1}{2}$ if T_i is a “vertical” tile (connected to the adjacent tiles through its horizontal sides) of type \boxplus , or if it is a horizontal tile of type \boxminus ;
- $\delta L_t = -\frac{1}{2}$ if T_i is a horizontal tile of type \boxplus or a vertical tile of type \boxminus .

Contribution of the flap tiles to L_t .

A flap tile can be covered by the ribbon either with four sections (three “bounces”) or none at all. In this latter case there is still a “bounce” of the ribbon when it goes from the previous tile to the next (superposed) tile: the ribbon travels from below the lower tile to above the upper tile or viceversa. We need to keep track of this extra bounce.

After analysing the possibilities we conclude for tile T_i as follows:

- $\delta L_t = +\frac{1}{2}$ if T_i is a vertical flap of type \boxplus (connected to the adjacent tile through a horizontal side), or if it is a horizontal flap of type \boxminus ;
- $\delta L_t = -\frac{1}{2}$ if T_i is a horizontal flap of type \boxplus or a vertical flap of type \boxminus .

Linking number of constructible configurations.

Theorem 4. *A constructible spatial configuration of the puzzle necessarily satisfies $L = 0$.*

Proof. The linking number L does not change under legitimate moves of the puzzle, so that it is sufficient to compute it on the initial configuration of Figure 1. There are no superposed tiles nor flaps, so that the ribbon does not cross itself, hence $L_c = 0$. The only contribution to L_t comes from the four straight tiles, and using the analysis of Section 6.2 it turns out that their contribution cancel one another so that also $L_t = 0$ and we conclude the proof. \square

Examples of configurations with nonzero linking number.

Due to Theorem 4 such configurations of the puzzle cannot be constructed.

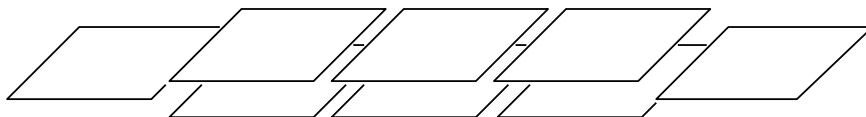


Figure 8: This configuration is not constructible because it has linking number $L \neq 0$.

One such configuration is shown in Figure 8 and would realize the maximal possible diameter for a configuration. The metric invariant of Section 5 is $\Delta = 0$ so that it is not enough to exclude this configuration, however we shall show that in this case $L \neq 0$ and conclude that we have a nonconstructible configuration. It will be studied in Section 9.

Another interesting configuration that can be excluded with the topological invariant and not with the metric one is a “figure eight” corresponding to the sequence (6) of Section 9. Figure 15 (right) show a 3D configuration that cannot be constructed because $L \neq 0$.

Octominoid configurations

A class of special configurations that can be studied using the two invariants introduced in Sections 5 and 6 consists of the so-called *octominoid* configurations. These correspond to positions of the eight tiles to form a 3D shape with all tiles parallel to one of the coordinate planes and no pair of superposed tiles. The term octominoid was introduced by Jürgen Köller in [2] and is suggested by the term *polyominoes* to denote planar shapes made of some fixed number of adjacent unit squares joined by their sides.

The total number of distinct octominoids is the large number 207265, most of which can be immediately excluded as possible configurations of the Rubik’s Magic because the eight squares cannot be cyclically connected by their sides; then a further reduction is obtained by enforcing the local constraints of Section 3.

The correct way of counting the set of feasible shapes (configurations of the undecorated puzzle that satisfy the local constraints) must take into account the cyclical ordering of the tiles together with the direction of their marked diagonals. It is thus possible to obtain the same 3D octominoid shape with different puzzle configurations: they come often in pairs, one configuration obtained from the other by reverting the direction of the diagonals, but there can be more than two configurations, or just one.

The total number of configurations in the shape of an octominoid that satisfy the local constraints turns out to be 1291 realizing a total of 582 different octominoid shapes.

These numbers are obtained by using a software code that can be downloaded from [\[4\]](#) and that will be briefly described in Section 11.1.

Any given octominoid configuration can be described by constructing the so-called *magic code*. It consists of a sequence of characters (like `RRmRRmRUmDUm`) with eight capital letters taken from the set `RLUD` (standing for *right*, *left*, *up*, *down*) optionally followed by the lower letter `m` (mountain fold) or `v` (valley fold).

They encode the relative adjacency information of each of the eight tiles with the next one. The first tile (say T_0) is oriented by drawing an arrow on one of its faces (front) parallel to a side. The selected orientation for T_0 **must** be such that the nylon strings cross the front face in the direction south-west to north-east (\boxtimes direction).

The first capital letter indicates which one of the four sides of T_0 is connected to T_1 (the subsequent tile), the presence of the lowercase `m` or `v` indicates that T_0 and T_1 form a 90 degrees angle either with a mountain fold (letter `m`) or with a valley fold with respect to the front face of T_0 . Otherwise T_1 is coplanar with T_0 .

The orientation of T_1 is compatible with the selected orientation of T_0 (as defined in Definition [\[1\]](#)), i.e. the drawn arrow on T_1 (in case of coplanarity) is exactly the mirror image of the arrow on T_0 with respect to the hinging side (the side of T_0 adjacent to T_1). As a simple example the starting 2×4 configuration of the puzzle can be encoded as `RRRURRRU` where it should be noted that the four tiles in the top row have downward arrows.

Since we are interested in configurations of the undecorated puzzle, many distinct magic codes describe the same configuration based on which tile we select as T_0 , how we orient it (such that T_0 becomes a \boxtimes tile) and in which direction we traverse the circular chain of eight tiles. The corresponding magic codes are all considered equivalent. A canonical magic code is then selected by taking all the disting equivalent magic codes and selecting the first one with respect to a suitable lexicographic ordering.

The lexicographic comparison is defined such that the four directions are ordered as $R < U < L < D$, and if the direction is the same, no fold is less than mountain fold which is less than a valley fold.

The mirror image of a constructible configuration can also be constructed by using the mirror images of the sequence of construction moves starting from the original 2×4 configuration, so that we also include all the magic codes of the mirror images in the same equivalence class.

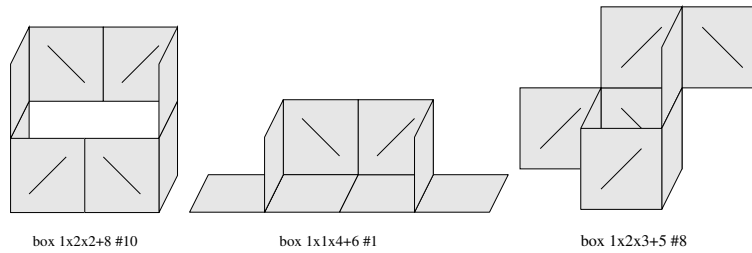


Figure 9: Examples of octominoid configurations. The label indicates the size of the smallest bounding box followed by $+k$ where k is the number of tiles that lie completely in the boundary of the bounding box. Finally $\#n$ is the sequential number in the table of the octominoid shapes in [4, 3D octominoid shapes].

Figure 9 shows three examples of octominoid configurations, the shape on the left is encoded by the magic code $\mathbf{RRmULmLLmURm}$, obtained by selecting as T_0 the lower-left front tile, oriented with an upward arrow in the visible face and traversing the configuration counterclockwise. Then tile T_1 is hinged at the right side of T_0 (hence the first \mathbf{R} character in the magic code) and is coplanar with T_0 (no \mathbf{m} or \mathbf{v} character following the first \mathbf{R}). Tile T_2 is also hinged at the right side of T_1 and tilted 90 degrees with a mountain fold (\mathbf{Rm}). Tile T_3 is hinged at the upper side of T_2 , note that the orientation of T_3 is consequently oriented with a downward arrow.

We have a number of equivalent magic codes by changing the choice and orientation of the starting tile, however the one coming first in the lexicographic ordering (the canonical magic code) is the string described above.

Similarly, the canonical magic code of the second image of Figure 9 is given by $\mathbf{RRRLmDvUDvLm}$, obtained by selecting as T_0 the leftmost tile. The third configuration of the figure is finally encoded by $\mathbf{RUUmLDvUvDmD}$ by suitably choosing and orienting the tile T_0 .

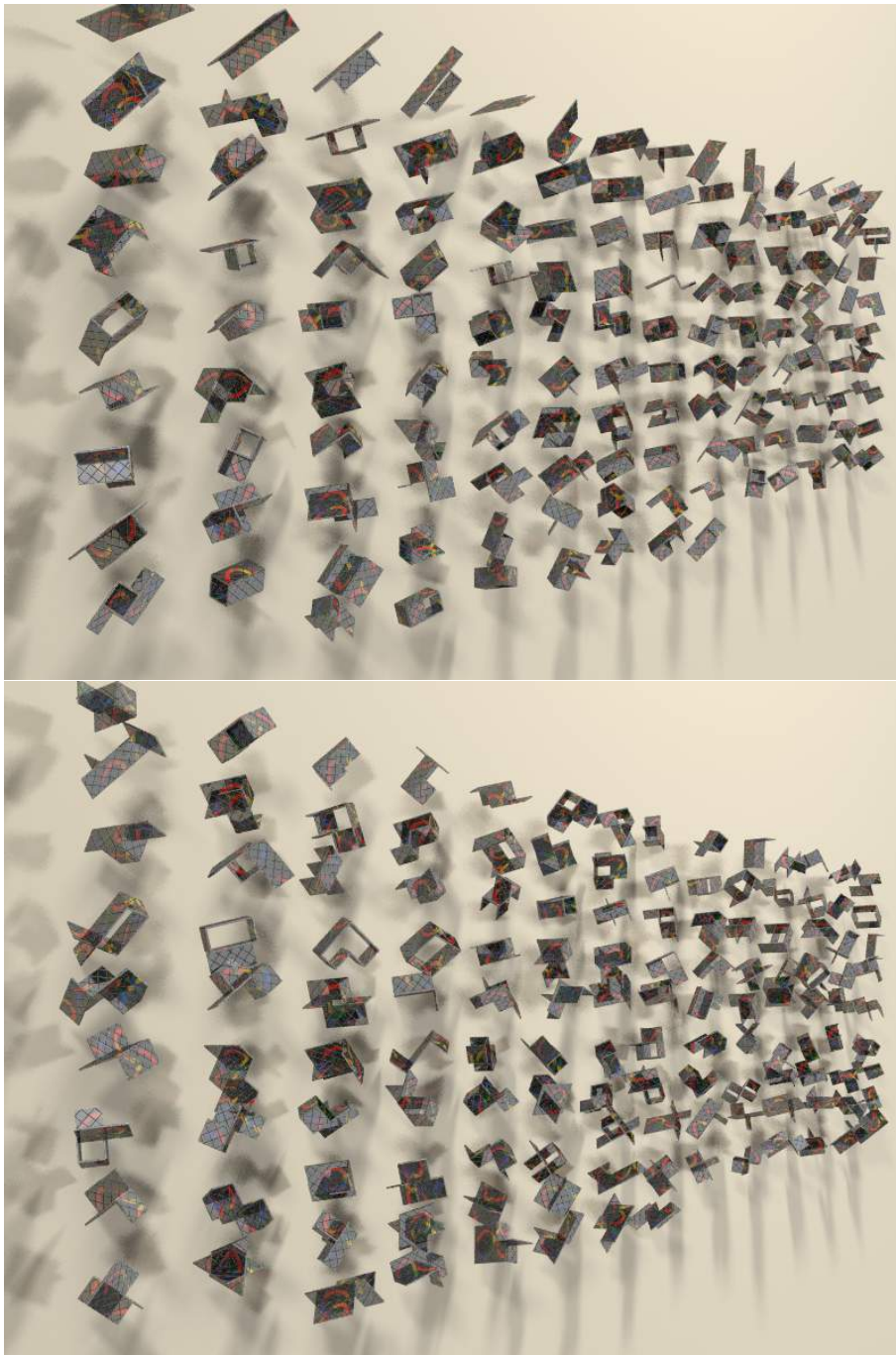


Figure 10: All 265 octominoid shapes with vanishing invariants. Synthetic images obtained with PovRay.

In the special class of octominoids, we were able to automate the computation of both the metric and the topological invariants of the configuration having a given magic code, thus allowing to quickly rule out all configurations with

nonzero invariants. Enforcing zero metric invariant reduces the configurations from 1291 down to 737, then enforcing also the vanishing of the linking number further reduces the number of configurations to 460 (265 distinct octominoid shapes).

These are all listed in [4, 3D octominoids], ordered according to the dimension of the smallest bounding box. Surprisingly, all of them could be actually constructed with the real puzzle, and building instructions are available in [4, 3D octominoids]. A few of such shapes are not present in the comprehensive table of symmetric 3D shapes in [2] and might be possibly obtained by us for the first time.

Figure 10 shows all 265 such shapes in one shot. The images were obtained synthetically using the ray-tracing software `PovRay`, in conjunction with the output of our software code to obtain the list of admissible magic codes.

Planar face-up configurations

We shall apply the results of the previous sections to a particular choice of spatial configurations, we shall restrict to planar configurations (all tiles parallel to the horizontal plane) with non-overlapping consecutive tiles. Superposed nonconsecutive tiles are allowed.

They can be obtained starting from strings of cardinal directions in the following way.

The infinite string $s : \mathbb{Z} \rightarrow \{E, N, W, S\}$ is a typographical sequence with index taking values in the integers \mathbb{Z} where the four symbols stand for the four cardinal directions East, North, West, South. On s we require

1. Periodicity of period 8: $s_{n+8} = s_n$ for any $n \in \mathbb{Z}$;
2. Zero mean value: in any subsequence of 8 consecutive characters (for example in $\{s_0, \dots, s_7\}$) there is an equal number of characters N as of characters S and of characters E as of characters W .

An **admissible sequence** is one that satisfies the two above requirements.

Periodicity allows us to describe an admissible sequence by listing 8 consecutive symbols, for definiteness and simplicity we shall then describe an admissible sequence just by listing the symbols s_1 to s_8 .

The character s_i of the string indicates the relative position between the two consecutive tiles T_{i-1} and T_i , that are horizontal and face-up.

The first tile T_0 can be of type \boxplus or type \boxminus , all the others T_i are of the same type as T_0 if i is even, of the opposite type if i is odd. The local constraints allows to recover a spatial configuration of the puzzle from an admissible sequence with two caveats:

1. For at least one of the tiles, say T_0 , it is necessary to specify if it is of type \boxtimes or \boxminus . We can add this information by inserting the symbol \boxtimes or \boxminus between two consecutive symbols, usually before s_1 ;
2. In case of superposed tiles (same physical position) it is necessary to clarify their relative position (which is above which). We can add this information by inserting a positive natural number between two consecutive symbols that indicates the “height” of the corresponding tile. In the real puzzle the tiles are not of zero width, so that their height in space cannot be the same. In case of necessity we shall insert such numbers as an index of the symbol at the left.

Remark 1 (Configurations that can be assembled). Given an admissible sequence it is possible to compute the number of superposed tiles at any given position. An **assemblage** of a sequence entails a choice of the height of each of the superposed tiles (if there is more than one). We do this by adding an index between two consecutive symbols. However for this assemblage to correspond to a possible puzzle configuration we need to require a condition. We hence say that an assemblage is **admissible** if whenever tile T_i is superposed to tile T_j , $i \neq j$, and also $T_{i\pm 1}$ is superposed to $T_{j\pm 1}$, then the relative position of the tiles in the two pairs cannot be exchanged. This means that if T_i is at a higher height than T_j , then $T_{i\pm 1}$ cannot be at a lower height than $T_{j\pm 1}$. It is possible that a given admissible sequence does not allow for any admissible assemblage or that it can allow for more than one admissible assemblage.

Observe that the mirror image of an oriented spatial configuration of the undecorated puzzle entails a change of type, \boxtimes tiles become of type \boxminus and viceversa. If the mirror is horizontal the reflected image is a different assemblage of the same admissible sequence with all tiles of changed type and an inverted relative position of the superposed tiles.

On the set of admissible sequences we introduce an equivalence relation defined by $s \equiv t$ if one of the following properties (or a combination of them) holds:

1. (cyclicity) The two sequences coincide up to a translation of the index: $s_n = t_{n+k}$ for all n and some $k \in \mathbb{Z}$;
2. (order reversal) $s_n = t_{k-n}$ for all n and some $k \in \mathbb{Z}$;
3. (rotation) s can be obtained from t after substituting $E \rightarrow N$, $N \rightarrow W$, $W \rightarrow S$, $S \rightarrow E$;
4. (reflection) s can be obtained from t after substituting $E \rightarrow W$ e $W \rightarrow E$.

Let us denote by \mathcal{S} the set of equivalence classes.

We developed a software code capable of finding a canonical representative of each of these equivalence classes, they are 71 (cardinality of \mathcal{S}). In Table [1](#) we summarize important properties of these canonical sequences, subdivided with respect to the number of flap tiles. It is worth noting that some of the 71 sequences admit more than one nonequivalent admissible assemblages in space due to the arbitrariness in choosing the type of tile T_0 and the ordering

of the superposed tiles. A few of the 71 admissible sequences do not admit any admissible assemblage, one of these is the only sequence with 8 flaps: $EW EW EW EW$. Since the constructability of a spatial configuration is invariant under specular reflection (which entails a change of type of all tiles) we can fix the type of tile T_0 , possibly reverting the order of the superposed tiles.

The canonical representative of an equivalence class in \mathcal{S} is selected by introducing a lexicographic ordering in the finite sequence s_1, \dots, s_8 where the ordering of the four cardinal directions is fixed as $E < N < W < S$. Then the canonical representative is the smallest element of the class with respect to this ordering.

The source of the software code can be downloaded from the web page [\[4\]](#).

Table 1: Sequences in \mathcal{S} .

number of flaps	number of sequences	number of assembl.	$\Delta = 0$ assembl.	$\Delta = L = 0$ assembl.	not classified
none	7	6	4	2	-
1	7	14	7	3	-
2	22	44	20	13	3
3	10	50	15	5	2
4	18	38	11	2	-
5	2	12	1	-	-
6	4	4	1	-	-
8	1	0	-	-	-
total	71	168	59	25	5

In Table [2](#) the sequences with two and four flaps are subdivided based on the distribution of the flaps in the sequence.

Theorem 5. *All planar face-up configurations have zero “twist” contribution to the topological invariant: $L_t = 0$. Consequently we have $L = L_c$ and to compute the linking number it is sufficient to compute the contributions coming from the crossing of the ribbon with itself. Any planar face-up configuration with an odd number of selfintersections of the ribbon with itself has $L \neq 0$.*

Proof. ^[1] We denote with k_1, \dots, k_s the number of symbols in contiguous subsequence of E, W (horizontal portions) or of N, S (vertical portions). Each portion of k_i symbols contains $k_i - 1$ straight tiles or flaps, all “horizontal” or “vertical”, hence each tile contributes to L_t with alternating sign due to the fact that the tiles are alternatively of type \boxplus and \boxminus . If $k_i - 1$ is even, then the contribution of this portion is zero, while if it is odd it will be equal to the contribution of the first straight or flap tile of the portion. It is not restrictive to assume that the first portion of k_1 symbols is horizontal and the last (of k_s symbols) is vertical. In this way if i is odd, then k_i is the number of symbols in a horizontal portion whereas if i is even, then k_i is the number of symbols in a vertical portion. Up to a change of sign of L_t we can also assume that the first

¹This proof is due to Giovanni Paolini, Scuola Normale Superiore of Pisa.

tile is of type \boxplus . Finally we observe that $k_i > 0$ for all i . Twice the contribution to L_t of the i -th portion is given by

$$(-1)^{i-1}(-1)^{k_1+k_2+\dots+k_{i-1}}(1+(-1)^{k_i}) \quad (2)$$

where the last factor in parentheses is zero if k_i is odd and is 2 if k_i is even; the sign changes on vertical portions with respect to horizontal portions (factor $(-1)^{i-1}$) and changes when the type (\boxplus or \boxminus) of the first straight or flap tile of the portion changes (factor $(-1)^{k_1+k_2+\dots+k_{i-1}}$). Summing up \boxplus on i and expanding we have

$$\begin{aligned} 2L_t &= \sum_{i=1}^s (-1)^{i-1}(-1)^{k_1+k_2+\dots+k_{i-1}} + \sum_{i=1}^s (-1)^{i-1}(-1)^{k_1+k_2+\dots+k_{i-1}}(-1)^{k_i} \\ &= -\sum_{i=1}^s (-1)^i(-1)^{k_1+k_2+\dots+k_{i-1}} + \sum_{i=1}^s (-1)^{i+1}(-1)^{k_1+k_2+\dots+k_i} \\ &= -\sum_{i=1}^s (-1)^i(-1)^{k_1+k_2+\dots+k_{i-1}} + \sum_{i=2}^{s+1} (-1)^i(-1)^{k_1+k_2+\dots+k_{i-1}} \\ &= 1 + (-1)^{s+1}(-1)^{k_1+k_2+\dots+k_s} = 0 \end{aligned}$$

because s is even and $k_1 + \dots + k_s = 8$, even. \square

Configurations with vanishing invariants

We shall identify admissible assemblages whenever they correspond to equivalent puzzle configurations, where we also allow for specular images. In particular this allows us to assume the first tile to be of type \boxplus .

Assemblages corresponding to non-equivalent sequences cannot be equivalent, on the contrary there can exist equivalent assemblages of the same sequence and this typically happens for symmetric sequences.

The two invariants can change sign on equivalent sequences or equivalent assemblages, this is not a problem since we are interested in whether the invariants are zero or nonzero. In any case the computations are always performed on the canonical representative.

The contribution Δ_c of $\Delta = \Delta_c + \Delta_f$ (coming from the curving tiles) can be computed on the sequence (it does not depend on the assemblage). On the contrary the contribution Δ_f coming from the flap tiles depends on the actual assemblage.

With the aid of the software code we can partially analyze each canonical admissible sequence and each of the possible admissible assemblages of a sequence. In particular the software is able to compute the metric invariant of an assemblage, so that we are left with the analysis of the topological invariant, and we shall perform such analysis only on assemblages having $\Delta = 0$, since our aim is to identify as best as we can the set of constructible configurations.

Sequences with no *flaps*

There are seven such sequences, three of them do not have any superposed tiles, so that they cover a region of the plane corresponding to 8 tiles (configurations of area 8). For these three sequences we only have one possible assemblage (having fixed the type \square of tile T_0).

The sequence

$$EEENWWWS \quad (3)$$

corresponds to the initial configuration 2×4 of the puzzle. The sequence

$$EENNWWSS \quad (4)$$

corresponds to the “window shape”, a 3×3 square without the central tile. The sequence

$$EENNWSWS \quad (5)$$

corresponds to the target configuration of the puzzle (Figure 2). Two sequences cover 7 squares of the plane (area 7), the sequence

$$EENWSSWN \quad (6)$$

and the sequence

$$ENENWSWS. \quad (7)$$

A sequence without flaps and area 6 (two pairs of superposed tiles) is

$$ENESWNWS. \quad (8)$$

The last possible sequence (with area 4) would be

$$ENWSENWS, \quad (9)$$

this however cannot be assembled in space since it consists of a closed circuit of 4 tiles traveled twice (see Remark 1).

The metric invariant is nonzero (hence the corresponding assemblage is not constructible) for the two sequences (4) and (7), the topological invariant L further reduces the number of possibly constructible configuration by excluding also the two sequences (6) e (8).

The remaining two configurations, corresponding to sequences (3) ed (5), are actually constructible (Figures 1 and 2).

Sequences with one *flap*

We find seven (nonequivalent) sequences with exactly one flap. Three of these have area 7:

$$EENNWSSW \quad (10)$$

$$EENWNSWS \quad (11)$$

$$EEENWWSW \quad (12)$$

and four have area 6:

$$EENWSWSN \quad (13)$$

$$EENWSWNS \quad (14)$$

$$EENWSNWS \quad (15)$$

$$EEENWSWW. \quad (16)$$

In all cases it turns out that there are two nonequivalent assemblages of each of these sequences according to the flap tile being ascending or descending, and they have necessarily a different value of Δ , so that at most one (it turns out exactly one) has $\Delta = 0$. We shall restrict the analysis of the topological invariant to those having $\Delta = 0$.

The two sequences (10) and (12) have $\Delta = 0$ if the (horizontal) flap tile is descending (Figure 4 right). The linking number reduces to $L = L_c$ (Theorem 5). Since in both cases we have exactly one crossing of the ribbon with itself we conclude that $L \neq 0$ and the sequences are **not constructible**.

To have $\Delta = 0$ the vertical flap of the sequence (11) must be descending. Then there is one crossing of the ribbon with itself, so that $L \neq 0$ and the configuration is **not constructible**.

Sequences (13) and (14) have $\Delta = 0$ provided their flap is ascending. We have now two crossings of the ribbon with itself and they turn out to have opposite sign in their contribution to L_c , so that $L = 0$ and the two sequences “might” be constructible.

Sequences (15) and (16) have $\Delta = 0$ provided their flap is ascending. Sequence (15) is then **not constructible** because there is exactly one selfcrossing of the ribbon so that $L = L_c \neq 0$. On the contrary, sequence (16) exhibits two selfcrossings with opposite sign and $L = L_c = 0$.

In conclusion of the 7 different sequences with one flap, four are necessarily non constructible because the topological invariant is non-zero, the remaining three sequences: (13), (14), (16) are actually constructible (refer to 4 planar face-up) for building instructions: first, second and third image of section “One flap”), see also Figure 11, first three images.

The two sequences with two adjacent *flaps*

Adjacency of the two flaps entails that both are ascending or both descending (Remark 1) and also they are both horizontal or both vertical since they are hinged to each other so that they contribute to the metric invariant $\Delta_f = \pm 4$ whereas $\Delta_c = 0$. Hence the metric invariant is nonzero and the two sequences are non-constructible.

The five sequences with two *flaps* separated by one tile

Sequence *EENWSEWW*

$\Delta = 0$ implies that the two (horizontal) flaps are one ascending and one descending. There are two non-equivalent admissible assemblages satisfying $\Delta = 0$, computation of the topological invariant gives $L = L_c = \pm 4$ for one of the two assemblages whereas the other has $L = L_c = 0$ and is actually constructible (Figure [12](#), second image):

$$\square E_3E_2NWS_2E_1W_1W. \quad (17)$$

For building instructions, see [4](#) [planar face-up], second image of section “Two flaps, area 5”.

Sequence *ENEWSNWS*

$\Delta = 0$ implies that both flaps (one is horizontal and one vertical) are ascending or both descending. The two corresponding distinct admissible assemblages have both $L = L_c = 0$. The two assemblages are:

$$\square E_2N_3EW_2S_2N_3WS \quad \text{and} \quad \square E_1N_1EW_2S_2N_3WS. \quad (18)$$

They are both constructible (Figure [12](#), third and first image respectively). For building instructions: [4](#) [planar face-up], third and first image of section “Two flaps, area 5”.

Sequence *ENEWSWS*

We can fix the first tile T_0 to be of type \square , then $\Delta_c = 4$ and $\Delta = 0$ implies that the first flap (horizontal) is ascending and the second (vertical) is descending. Computation of the topological invariant gives $L = L_c = 0$ and we have another unclassified sequence:

$$\square EN_1EW_3NS_2WS.$$

The two lowest superposed tiles can be exchanged, however the resulting assemblage is equivalent due to the reflection symmetry of the sequence of symbols.

Sequence *ENWESNWS*

Imposing $\Delta = 0$ the two flaps (one is horizontal and one is vertical) must be both ascending or both descending. In both cases we compute $L = L_c = 0$. Actually the two assemblages are equivalent by taking advantage of the symmetry of the sequence, one of these is

$$\square E_1N_1W_1E_2S_2N_3W_2S \quad (19)$$

and is constructible (Figure [12](#), fourth image); building instructions in [4](#) [planar face-up], image in section “Two flaps, area 4”.

Sequence $EENWSSNW$

Imposing $\Delta = 0$ the two flaps (one horizontal and one vertical) must be both ascending or both descending. In both cases we compute $L = L_c = 0$. The two assemblages are equivalent as in the previous case, one of these (Figure 11, 8-th image) is

$$\square E_1ENWS_3SN_2W \tag{20}$$

and building instructions can be found in [4, planar face-up], fifth image of section “Two flaps, area 6”.

The three sequences with two flaps separated by two tiles

All three admissible sequences with two flaps at distance 3 (separated by two tiles) have $\Delta_c = 0$. Two of these sequences have both horizontal or both vertical flaps, so that $\Delta = 0$ entails that one flap is ascending and one is descending. The third sequence has an horizontal flap and a vertical flap so that $\Delta = 0$ entails that both flaps are ascending or both descending. In all cases we have two selfcrossings of the ribbon with opposite sign, hence $L = L_c = 0$ and might be constructible. Each of the three sequences admit two distinct assemblages both with $\Delta = L = 0$:

$$\square E_2E_2EW_1NWS_1W \quad , \quad \square E_1E_1EW_2NWS_2W \tag{21}$$

$$\square E_2ENW_1NS_2S_1W \quad , \quad \square E_1ENW_2NS_1S_2W \tag{22}$$

$$\square E_2ENW_2WE_1S_1W \quad , \quad \square E_1ENW_1WE_2S_2W \tag{23}$$

The first two and the last two are actually constructible (Figure 11, 4-th, 5-th, 6-th and 7-th image respectively); building instructions in [4, planar face-up], images 1 to 4 of section “Two flaps, area 6”. The first of the second row is also constructible (Figure 11, 9-th image) although with a considerable amount of strain on the nylon wires. Building instructions in [4, planar face-up], 6-th image of section “Two flaps, area 6”.

The twelve sequences with two flaps in antipodal position

Table 2: Sequences with two flaps (left) and four flaps (right) subdivided based on the relative position of the flaps.

sequences with 2 flaps	distribution of flaps	sequences	dist. of flaps
2	ffxxxxxx	1	ffffxxxx
5	fxfxxxxx	5	fffxxfxx
3	fxxfxxxx	1	ffxffxxx
12	fxxxfxxx	4	ffxfxfxf
		1	ffxxffxx
		6	fxfxfxfx

Of the 12 sequences with two flaps in opposite (antipodal) position we first analyze those (they are 10) in which the tiles follow the same path from one flap to the other and back. One of these is shown in Figure 8. All have $\Delta_c = 0$

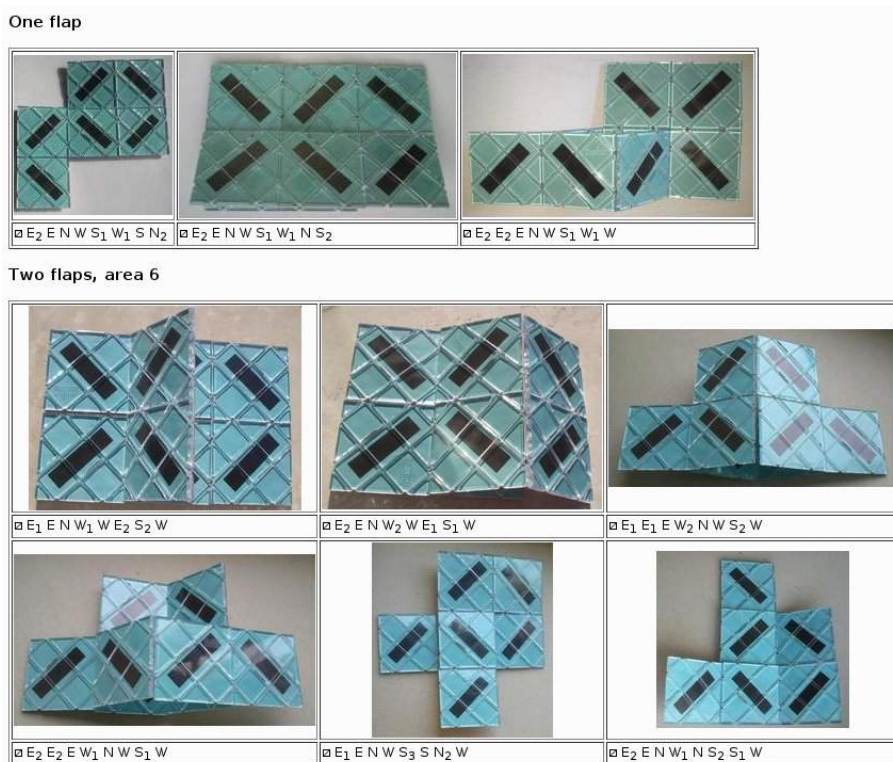


Figure 11: The three constructible configurations with one flap and those with two flaps and area 6. For building instructions we refer to [4], click on “planar face-up”.

so that the contribution of the two flaps must have opposite sign in order to have $\Delta = 0$. If one flap is horizontal and the other vertical, then they must be both ascending or both descending and we have no possible admissible assemblage (Remark 1). We are then left with those sequences having both horizontal or both vertical flaps, one ascending and one descending. In this situation we find that the ribbon has 3 selfcrossings, so that necessarily $L = L_c \neq 0$ and these sequences are also not constructible.

We remain with the two sequences $EENEWWWSW$ and $EENNSWSW$ that both have a contribution $\Delta_c = -4$ (fixing T_0 of type \square), so that the two flaps must contribute with a positive sign to the metric invariant. The first sequence has both horizontal flaps, and they must be both descending, this is now possible thanks to the different path between the two flaps. The second sequence has one horizontal and one vertical flap, so that the first must be ascending and the second descending. There are exactly two selfcrossings of the ribbon in both cases, however they have the same sign in the first case implying $L = L_c \neq 0$, hence non constructible. They have opposite sign in the second case and we have both zero invariants. In conclusion the only one of the 12 sequences that might be constructible is

$$\square E_1 E N_1 N S_2 W S_2 W. \quad (24)$$

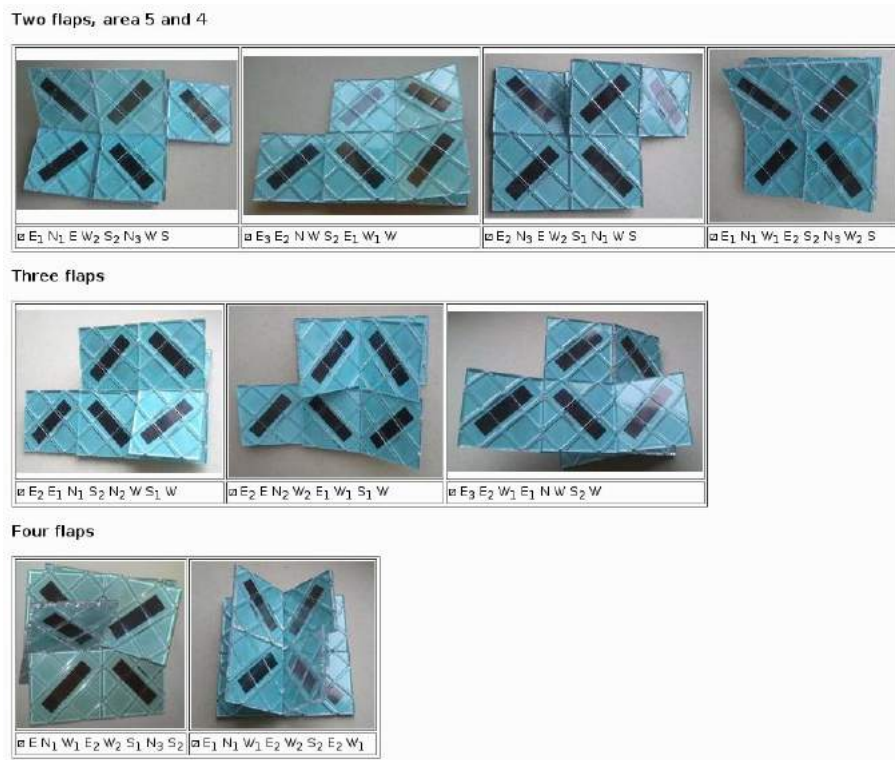


Figure 12: Constructible configurations with two flaps, area 5 and 4 and configurations with three and four flaps. For building instructions we refer to [4], click on “planar face-up”.

Sequences with three *flaps*

Of the 10 admissible sequences with three flaps there is only one with all adjacent flaps, having $\Delta_c = \pm 2$. The three flaps being consecutive are all horizontal or all vertical and all ascending or all descending, with a total of $\Delta_f = \pm 6$ and the metric invariant cannot be zero.

Four sequences have two adjacent flaps, and in all cases $\Delta_c = \pm 2$. Imposing $\Delta = 0$ allows to identify a unique assemblage for each sequence (with one exception). In all cases a direct check allows to compute $L = L_c = 0$. These sequences are:

$$\square E_3 E_2 W_{1,2} E_1 N W S_{2,1} W \quad , \quad \square E_3 E N W_1 S_1 N_2 S_2 W \quad (25)$$

$$\square E_2 E N_2 W_2 E_1 W_1 S_1 W \quad , \quad \square E_2 E_1 N_1 S_2 N_2 W S_1 W. \quad (26)$$

The last two are actually constructible (Figure [12] 5-th and 6-th images), building instructions in [4] planar face-up], first and second images of section “Three flaps”. One of the two assemblages of the left sequence in (25) can be actually constructed (Figure [12] 7-th image), building instructions in [4] planar face-up], third image of section “Three flaps”. If the puzzle had sufficiently deformable nylon threads and tiles we could conceivably deform the first

assemblage into the second. We do not know at present if the right sequence in (25) is constructible (unclassified).

The five remaining sequences all have $\Delta_c = \pm 2$. Imposing $\Delta = 0$ leaves us with 10 different assemblages: the sequence with all three horizontal flaps has three different assemblages with $\Delta = 0$, three of the remaining four sequences (with two flaps in one direction and the third in the other direction) have two assemblages each, the remaining sequence has only one assemblage with $\Delta = 0$. In all cases a direct check quantifies in 3 or 5 (in any case an odd value) the number of selfcrossings of the ribbon, so that $L = L_c \neq 0$. None of these sequences is then constructible.

Sequences with four *flaps*

There are 18 such sequences. Six of these have a series of at least three consecutive flaps and a contribution $\Delta_c = 0$. They are not constructible because the consecutive flaps all contribute with the same sign to Δ_f .

The sequences $ENWEWSNS$ and $ENWEWSEW$ have $\Delta_c = 0$ and two pairs of adjacent flaps oriented in different directions in the first case and in the same direction in the second case. To have $\Delta = 0$ they must contribute with opposite sign and hence must be all ascending or all descending in the first case whereas in the second case one pair of flaps must be ascending and one descending. Thanks to the symmetry of the sequences the two possible assemblages of each are actually equivalent. The linking number turns out to be $L = 0$ and we have two possibly constructible configurations:

$$\boxtimes EN_1W_1E_2W_2S_1N_3S_2 \quad \text{and} \quad \boxtimes E_1N_1W_1E_2W_2S_2E_2W_1. \quad (27)$$

Both turn out to be constructible (Figure 12, 8-th and 9-th images), building instructions in [4, planar face-up], images of section “Four flaps”.

There are four sequences with a single pair of adjacent flaps, the other two being isolated, all with $\Delta_c = 0$. The two isolated flaps must contribute to the metric invariant with the same sign, opposite to the contribution that comes from the two adjacent flaps. In three of the four cases the two isolated flaps have the same direction and hence both must be ascending or both descending. It turns out that there is no admissible assemblage with such characteristics. The pair of adjacent flaps of the remaining sequence ($ENSWWW$) are horizontal. If they are ascending the remaining horizontal flap must be descending whereas the vertical flap must be ascending (to have $\Delta = 0$). This situation (or the one with a descending pair of adjacent flaps) is assemblable and we can compute the linking number, which turns out to be $L = L_c = \pm 2$. Even this configuration is not constructible.

The remaining six sequences (flaps alternating with non-flap tiles) all have the non-flap tiles superposed to each other. An involved reasoning, or the use of the software code, allows to show that for two of this six sequences, having area 3, namely $EEWWEWW$ and $ENSWENSW$, there is no possible admissible assemblage with $\Delta = 0$.

Sequence *ENSEWNSW*

This sequence has area 4, with two of the four flaps superposed to each other. Using the software code we find two different assemblages having $\Delta = 0$.

Computation of the linking number leads in both cases to $L = L_c = \pm 2$, hence this sequence is not constructible.

Sequence *EEWNSEWW*

This sequence has also area 4, with two of the four flaps superposed to each other. Using the software code we find only one assemblage having $\Delta = 0$.

Computation of the linking number leads in to $L = L_c = \pm 2$, hence this sequence is also not constructible.

Sequence *EWNSSNW*

This sequence has area 5 with no superposed flaps and contribution $\Delta_c = 0$, so that to have $\Delta = 0$ two flaps contribute positively and two contribute negatively to the metric invariant.

The software code gives three different assemblages with $\Delta = 0$.

An accurate analysis of the selfcrossings of the ribbon due to the flaps shows that flaps that contribute positively to the metric invariant also contribute with an odd number of selfcrossings of the ribbon, besides there is one selfcrossing due to the crossing straight tiles.

In conclusion we have an odd number of selfcrossings, hence the sequence is not constructible.

Sequence *ENSEWSNW*

This sequence has also area 5 with no superposed flaps, but now the contribution of the curving tiles to the metric invariant is $\Delta_c = 4$, so that to have $\Delta = 0$ exactly one of the flaps has positive contribution to the metric invariant. This flap will also contribute with an odd number of selfcrossings of the ribbon. In this case there are no other selfcrossings of the ribbon because there are no straight tiles, so that we again conclude that the number of selfcrossings of the ribbon is odd and that $L = L_c \neq 0$. This sequence is also not constructible.

Sequences with five *flaps*

Both sequences have $\Delta_c = -2$.

The software code quickly shows that the sequence *EEWNSNSW* does not have any admissible assemblage with $\Delta = 0$.

The other sequence is $EEWEWNSW$ and to have $\Delta = 0$ the three consecutive horizontal flaps must be ascending, and also the vertical flap must be ascending. There is one admissible assemblage satisfying these requirements, but the resulting number of selfcrossings of the ribbon is odd, and so also this configuration is not constructible.

Sequences with six *flaps*

None of the four sequences with six flaps is constructible. Indeed it turns out that all have $\Delta_c = 0$, so that in order to have $\Delta = 0$ they must have three flaps with positive contribution and three with negative contribution to Δ_f .

Two of the four sequences have four or more flaps that are consecutive and hence all contribute with the same sign to Δ_f , so that $\Delta \neq 0$.

The sequence $EEWEWWEW$ must have three ascending consecutive flaps and three consecutive descending flaps (all flaps are horizontal). Analyzing the ribbon configuration shows that there are an odd number of ribbon selfcrossings, hence $L = L_c \neq 0$.

Finally, all the six flaps of sequence $ENSNSWEW$ must be ascending in order to have $\Delta = 0$, there is no admissible assemblage with this property.

Sequences with seven *flaps*

There is none.

Sequences with eight *flaps*

The only one is $EWWEWEWEW$, but there is no admissible assemblage of this sequence.

Unclassified configurations

Sequences with two *flaps*

There are 3 unclassified assemblages, corresponding to 3 sequences. The assemblage

$$\square EN_1EW_3NS_2WS$$

has two flaps separated by one tile.

This assemblage of the sequence (22, right) has two flaps separated by two tiles:

$$\square E_1ENW_2NS_1S_2W.$$

Finally there is one unclassified assemblage with two tiles separated by three tiles:

$$\square E_1 E N_1 N S_2 W S_2 W. \tag{28}$$

A schematic visualization of these assemblages is depicted in Figure 13

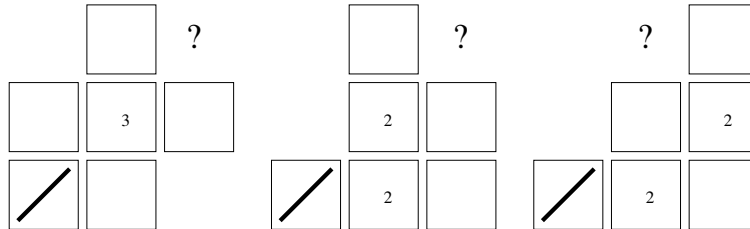


Figure 13: Schematic structure of the three unclassified sequences with two flaps.

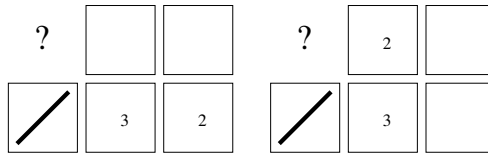


Figure 14: Schematic structure of the two unclassified sequences with three flaps.

Sequences with three flaps

There are 2 of them:

$$\begin{aligned} &\square E_3 E_2 W_2 E_1 N W S_1 W \\ &\square E_3 E N W_1 S_1 N_2 S_2 W. \end{aligned}$$

The first one would conceivably be constructible starting from $\square E_3 E_2 W_1 E_1 N W S_2 W$ by exchanging the position of two tiles, which is possible only with a very large amount of stretching on the wires and deformation of the tiles, not available on the real puzzle.

A schematic visualization of these assemblages is depicted in Figure 14

The software codes

The software code is contained in the Subversion (svn) repository [5], together with a povray module that can be used to produce syntetized images of 3D configurations and scripts to produce a printout with customized decorations for the puzzle. The code can also be downloaded from [4] and should work on any computer with a C compiler.

There are actually two distinct software codes, described in Section 11.1 (octominoid shapes) and Section 11.2 (planar face-up configurations).

3D octominoid shapes

The name of the executable is `rubiksmagic`. If run without arguments, it will search for all canonical representatives of the set of octominoid configurations that satisfy the local constraints (feasible configurations), using the *magic code* described in Section 7.

This is part of its output:

```

$
./rubiksmagic

RRRURRRU box=0x2x4+8 polyominoid=011-013-015-017-031-033-035-037s
      f=0 delta=0 linking=0 symcount=4 typeinv=yes
RRRUMRRRUM box=1x1x4+8 polyominoid=011-013-015-017-101-103-105-107s
      f=0 delta=0 linking=0 symcount=4 typeinv=no
[...]
RmUvRvLmUvUmUvLv box=2x2x2+0 polyominoid=112-...-312
      f=4 delta=4 linking=0 symcount=1 typeinv=no
RmUvUmLvRmUvUmLv box=2x2x2+0 polyominoid=112-...-323s
      f=4 delta=0 linking=0 symcount=4 typeinv=yes
Found 1291 sequences
$

```

The output actually consists of a single (long) line for each configuration, here wrapped in two lines for convenience, and contains the following information.

box The bounding box of the octominoid shape with syntax $xyxz+t$ where x , y , z are the dimensions of the smallest box that contains the shape (rotated such that $x \leq y \leq z$). The special boxes $0x2x4$ and $0x3x3$ correspond to the two basic flat octominoid configurations, apart from these, we have exactly eight distinct boxes: $1x1x2$ (colored purple in [2]), $1x1x3$ (green), $1x1x4$ (blue), $1x2x2$ (red), $1x2x3$ (grey), $1x3x3$ (dark grey), $2x2x2$ (light blue), $2x2x3$ (yellow). The number following the + sign $0 \leq t \leq 8$ denotes the number of tiles of the configuration that lie at the boundary of the bounding box;

polyominoid Describes the actual 3D shape, there is a sequence of eight groups of triplets of digits. Each group describes the 3D position of a tile as follows: observe that in each group exactly one of the three digits is even, after dividing all digits by two we obtain the 3D coordinates of the center of the tile. This uniquely determines the orientation of the tile by observing that the only integral coordinate indicates the direction of the normal vector to the tile;

f The number of flaps in the configuration;

delta This is the computed value of the metric invariant introduced in Section 5;

linking This is the computed linking number L (topological invariant) introduced in Section 6;

symcount The order of the group of symmetries. For example, a configuration that is mirror symmetric will have **symcount** at least two (Figure 9, center, is an example). The possible values are 1, 2, 4, 8. The configuration of Figure 9 (right) is completely unsymmetric, hence **symcount** is 1. There are 4 configurations with the maximal value 8 for **symcount**, but only one of these: `RRmRRmRRmRRm` has both vanishing invariants and has the shape of the lateral surface of a square prism of side 2 and height 1. Because of the marked diagonals of the tiles, this configuration is **not** symmetric with respect to reflection about an intermediate plane parallel to the base of the prism, thus reducing the number of symmetries from 16 (symmetries of a square prism) to 8;

typeinv Usually, exchanging the type of all the tiles from \square to \boxtimes and viceversa produces a non-equivalent configuration (**typeinv=no**). However, 141 of the 1291 feasible configurations produce an equivalent configuration upon such exchange (**typeinv=yes**), 50 of them have vanishing invariants. One of these is shown in Figure 9 (left).

It is clear from the description above that the software code is able to compute both invariants (in contrast with the code for the planar face-up configurations described in the next subsection, for which the code is currently not able to compute the linking number).

Using option `-M` (`./rubiksmagic -M`) has the effect of filtering out all configurations with nonvanishing metric invariant ($\Delta \neq 0$). Similarly option `-T` filters out configurations with nonvanishing topological invariant ($L \neq 0$).

Option `-w` allows to display the warp code described by Verhoeff in [7]; a few other options are described by `./rubiksmagic --help`.

The `rubiksmagic` command accepts an argument, in the form of a magic code, in which case the computation is limited to the corresponding configuration: the code first computes the canonical (equivalent) magic code and displays all the above informations for that configuration.

Finally, the code is not limited to the case of the puzzle with eight tiles; option `-n` n can be use to compute with the puzzle with n tiles (n must be even).

As an example, the configuration having magic code `RmRvUvDmLvLmDmUv` (Figure 15, left) is analyzed as

```

$
./rubiksmagic

RmRvUvDmLvLmDmUv box=2x2x2+2 polyominoid=011-112-121-...-433s
      f=0 delta=-4 linking=0 symcount=2 typeinv=yes
$

```

where option `-c` inhibits the canonization of the magic code. Since $\Delta \neq 0$ such configuration cannot be constructed.

The configuration with magic code `RRRmRmRRLmLm` (Figure 15, right) is analyzed as

```

$
./rubiksmagic

RRRmRmRRLmLm box=1x1x3+7 polyominoid=011-013-015-110-114-211-213-215s
      f=2 delta=0 linking=1 symcount=2 typeinv=yes
$

```

and is not constructible since the topological invariant $L = 1$ does not vanish.

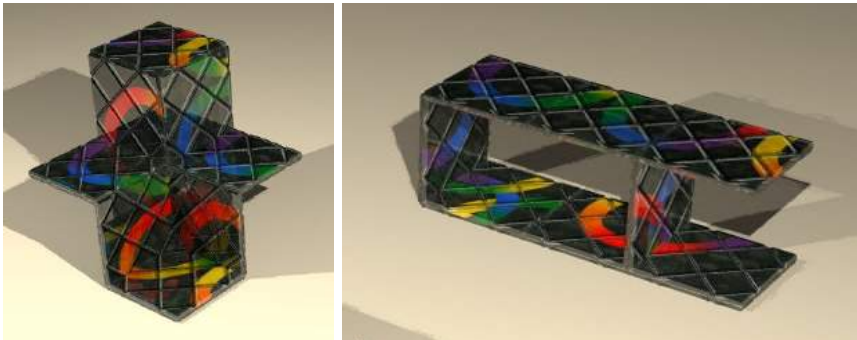


Figure 15: The configuration on the left has magic code `RmRvUvDmLvLmDmUv`. The configuration on the right has magic code `RRRmRmRRLmLm`. These computer generated images were obtained from the magic codes of the configurations using the PovRay raytracing program and the include file provided in [5].

Planar face-up shapes

The name of the executable is `rubiksmagic2d`. If run without arguments, it will search for all canonical representatives of the set \mathcal{S} of equivalent classes of sequences.

This is part of its output:

```

$
./rubiksmagic

EEEEWWW f=2 area=5 Dc=0 symcount=8 assemblages=1 deltaiszero=1
EEENWWWS f=0 area=8 Dc=0 symcount=4 assemblages=1 deltaiszero=1
EEENWSW f=1 area=7 Dc=-2 symcount=1 assemblages=2 deltaiszero=1
[...]
ENSWNSW f=4 area=3 Dc=0 symcount=8 assemblages=0 deltaiszero=0
EWEWEW f=8 area=2 Dc=0 symcount=32 assemblages=0 deltaiszero=0
Found 71 sequences
$

```

It searches for all admissible sequences that are the canonical representative of their equivalent class in \mathcal{S} (it finds 71 equivalent classes), for each one it prints the sequence followed by some information (to be explained shortly).

The software allows for puzzles with a different number of tiles, for example for the large version with 12 tiles of the puzzle it finds 4855 equivalence classes, with a command like

```

$
./rubiksmagic

EEEEEEWWWWW f=2 area=7 Dc=0 symcount=8 assemblages=1 deltaiszero=1
EEEEENWWWWWS f=0 area=12 Dc=0 symcount=4 assemblages=1 deltaiszero=1
EEEEENWWWWWSW f=1 area=11 Dc=-2 symcount=1 assemblages=2 deltaiszero=1
[...]
ENSNWNSNSW f=8 area=3 Dc=0 symcount=4 assemblages=0 deltaiszero=0
ENSNWNSWEW f=8 area=3 Dc=0 symcount=2 assemblages=0 deltaiszero=0
ENSWNSWNSW f=6 area=3 Dc=0 symcount=12 assemblages=0 deltaiszero=0
EWEWEWEWEW f=12 area=2 Dc=0 symcount=48 assemblages=0 deltaiszero=0
Found 4855 sequences
$

```

However the computational complexity grows exponentially with the number of tiles.

Another use of the code allows to ask for specific properties of a given sequence, we illustrate this with an example:

```

$
./rubiksmagic

EEWENWSW f=3 area=5 Dc=-2 symcount=1 assemblages=6 deltaiszero=2
  Assemblage with delta = 0: sla E3 E2 W2 E1 N1 W1 S1 W1
  Assemblage with delta = 0: sla E3 E2 W1 E1 N1 W1 S2 W1
$

```

The first line of output displays some information about the sequence given in the command line, specifically we find

- the sequence itself;
- the number of flaps (3 in this case);
- the area of the plane covered (5);
- the computed contribution Δ_c coming from the curving tiles;
- the cardinality of the group of symmetries of the sequence, this particular sequence does not have any symmetry;
- the number of admissible assemblages of the sequence, counting only those that start with T_0 of type \square and identifying assemblages that are equivalent under transformations in the group of symmetries of the sequence;
- the number of admissible assemblages with vanishing metric invariant ($\Delta = 0$), we have two in this case.

Then we have one line for each of the possible assemblages with $\Delta = 0$ with a printout of each assemblage, the numbers after each cardinal direction tells the level of the tile reached with that direction. It will be 1 for tiles that are not superposed with other tiles, otherwise it is an integer between 1 and the number of superposed tiles.

The option ‘-c’ on the command line can be omitted in which case the software computes the canonical representative of the given sequence and prints all the informations for both the original sequence and the canonical one. Note that the sign of the invariants is sensitive to equivalence transformations.

References

- [1] Rubik’s Magic - *Wikipedia*, https://en.wikipedia.org/wiki/Rubik's_Magic, retrieved Jan 15, 2014.
- [2] Köller, J.. Rubik’s Magic, <http://www.mathematische-basteleien.de/magics.htm>, retrieved Jan 15, 2014.
- [3] Nourse, J.G. *Simple Solutions to Rubik’s Magic*, New York, 1986.
- [4] Paolini, M. Rubik’s Magic, <http://rubiksmagic.dmf.unicatt.it/>, retrieved Jan 15, 2014.
- [5] Paolini, M. rubiksmagic project, Subversion repository, 2015, <https://svn.dmf.unicatt.it/svn/projects/rubiksmagic/trunk>.
- [6] Scherphuis, J. Rubik’s Magic Main Page, <http://www.jaapsch.net/puzzles/magic.htm>, retrieved Jan 15, 2014.
- [7] Verhoeff, T. “Magic and Is Nho Magic”, *Cubism For Fun*, 15, 24–31, 1987.